

# Fundamentals of Liquid Phase Sintering Related to Selective Laser Sintering

D.E. Bunnell, D.L. Bourell, and H.L. Marcus

The Center for Materials Science  
University of Texas at Austin

## Abstract

Liquid phase sintering is one of the underlying principles that must be modeled and understood when the Selective Laser Sintering (SLS) process is used. This paper describes the initial studies being conducted to measure surface tension of metal alloys used for SLS. A low melting point solder was used to verify the wetting balance and pendant drop techniques and equipment for determining surface tension. The liquid-solid, liquid-vapor, and solid-vapor surface tension of 80 Sn - 20 Pb solder on mild steel was determined to be 245, 417, and 662 dynes/cm.

## Introduction

Selective Laser Sintering (SLS) is a process that uses a rastering laser to sinter powder particles into a computer defined shape. Because the laser is typically rastered at speeds of 1 to 10 cm per second, the particles under the laser spot may only be at sintering temperatures for a few seconds. If the particles are to be sintered during this short period, either melting or a chemical reaction must occur to form particle necks. Liquid phase sintering (LPS) differs from conventional sintering in that a liquid phase allows for particle rearrangement and contact dissolution which accelerates the initial shrinkage rate and is the underlying principle of SLS processing of two phase (low and high melting point alloys) systems.

To evaluate the phenomena that control LPS during SLS, several factors must be considered: the rate with which a molten metal will wet a solid metal, the surface tension of liquid-solid and liquid-vapor interfaces, the dissolution rate of the solid phase in the liquid phase, the temperature transition of a powder bed as the laser rasters over it, modeling of the initial particle rearrangement during liquid phase sintering, and applying the model to fabricate a multilayer metal part using SLS. Results of the initial studies of these factors will be presented here.

## Liquid Phase Sintering Theory

Kingery proposed three stages for liquid phase sintering<sup>1</sup>. The first stage is the formation of a liquid phase which flows and facilitates the rearrangement of particles. The second stage occurs when the liquid phase dissolves the solids and the compact density increases by solution and reprecipitation. The final phase is the formation of a solid skeleton as the compact become homogeneous and the melting point of the liquid exceeds the processing temperature.

The first stage of liquid phase sintering, particle rearrangement, results in the most rapid and largest extent of densification<sup>2,3</sup>. During SLS, the only part of the powder bed that contains liquid is the small area directly under the moving laser beam and the small area trailing the current position that

has not cooled below the melting point of the liquid phase. These areas will only experience a molten second phase for a short period of time, of the order of seconds, before being cooled to the temperature of the surrounding solid material. Therefore, it behooves us to model the liquid phase sintering particle rearrangement kinetics so as to characterize SLS.

During the initial stage of LPS the mechanism for densification is particle rearrangement driven by surface tension forces<sup>4</sup>. Kingery proposed that the densification of the compact could be modeled by the equation<sup>5</sup>:

$$\frac{\Delta V}{V} = \frac{-27 C_n \gamma_{lv}^2 t^2}{16 r^2 \eta^2}$$

Where V is the volume of the compact,  $C_n$  is the coordination number,  $\gamma_{lv}$  is the liquid-vapor surface tension, t is time, r is the particle radius, and  $\eta$  is the melt viscosity. From this equation, we need to find  $\gamma_{lv}$ , the liquid-vapor surface tension, and  $\eta$ , the liquid viscosity.

The driving force for liquid phase sintering is the capillary force that a wetting liquid exerts between two solids<sup>6,7</sup>. The capillary force consists of two components, surface tension and a pressure difference due to the meniscus curvature. To determine the capillary forces, it is necessary to find  $\gamma_{ls}$  and  $\gamma_{sv}$ , the liquid-solid and solid-vapor surface tensions.

The kinetics of wetting are not completely understood. The reactions preceding the advancing liquid front that are responsible for oxide layer removal are complex and involve diffusion of metal vapors through pores in the oxide and changes in surface tension due to surface active elements. Since wetting of metal particles is required for liquid phase sintering during SLS, the kinetics of wetting need to be determined to model this process.

The wetting balance test provides information on the transient wetting characteristics of a liquid-solid couple<sup>8</sup>. Figure 1 is a sketch of the three stages that a solid sample experiences during a wetting balance test. During the initial immersion of the solid into the molten metal, the sample is not wet and is lifted by the surface tension of the liquid. Within a fraction of a second, the liquid starts to react with the surface layer and begins to wet the exposed surface of the solid. The third stage is when the equilibrium meniscus has formed.

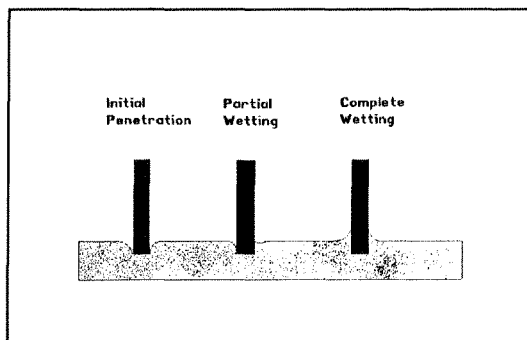


Figure 1. Stages of wetting during wetting balance test.

The value of  $\gamma_{ls}$  (the liquid-solid surface tension) can be determined from a force balance that includes three terms, the weight of the meniscus around the perimeter of the sample, the surface tension that pulls the liquid up, and a buoyancy term related to the volume of liquid displaced:

$$\Sigma F_y = 0 = (\Delta wt \cdot g)/l - \gamma_{ls} / \cos\theta + \Delta\rho \cdot V_d$$

Where  $\Delta wt$  is the weight increase of the sample,  $g$  is the gravitational constant,  $l$  is the perimeter of the sample,  $\theta$  is the contact angle of the liquid-solid interface,  $\Delta\rho$  is the difference in density between the solid and liquid, and  $V_d$  is the volume of liquid displaced.

If the sample penetration into the liquid is small, the buoyancy term can be neglected and from the force balance,  $\gamma_{ls}$  is given by the relationship:

$$\gamma_{ls} = (\Delta wt \cdot g)/l \cdot \cos\theta \quad (1)$$

The liquid-vapor surface tension ( $\gamma_{lv}$ ) can be determined by measuring the weight of a pendant drop<sup>9</sup>. Figure 2 is a sketch of a pendant drop showing the two curvatures. As a drop forms at the end of a rod, two curvatures control when it will separate. If the drop is small, gravity may be neglected and the curvatures of the pendant drop are related to the surface tension by the Laplace equation<sup>10</sup>:

$$\Delta P = \gamma_{lv} 2H$$

where  $2H$  is the Gaussian average curvature and  $\Delta P$  is the pressure difference. For a symmetrical drop where both curves are revolutions about an axis, the average curvature is given by:

$$2H = (1/R_1 + 1/R_2)$$

In practice, an empirical relationship exists between the diameter of the rod and  $2H$ . The surface tension can be calculated as:

$$\gamma_{lv} = m \cdot g \cdot F/R_1 \quad (2)$$

where  $m$  is the mass of the drop,  $g$  is the gravitational constant,  $F$  is the correlation factor related to  $r/V^{1/3}$  (where  $V$  is the volume of the drop after it has separated from the rod), and  $R_1$  is the radius of the solid rod.

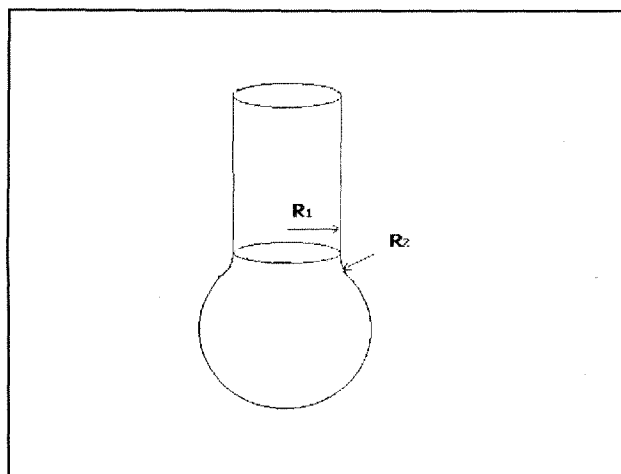


Figure 2. Curvature on a pendant drop

The factor "F" is empirically fitted to the equation:

$$F = 0.14782 + 0.27896(r/V^{1/3}) - 0.166(r/V^{1/3})^2 \quad (3)$$

Where V is the volume of a drop.

To determine the solid-vapor surface tension,  $\gamma_{sv}$ , the contact angle of the solidified metal was measured. At equilibrium, the condition for a liquid to wet a solid is given by Young's equation<sup>11</sup>:

$$\gamma_{sv} = \gamma_{ls} + \gamma_{lv} \cos \theta \quad (4)$$

Since  $\gamma_{ls}$  and  $\gamma_{lv}$  are measured using the wetting balance and the pendant drop tests, to find  $\gamma_{sv}$  all that is needed is the contact angle  $\theta$ .

### Equipment

A "wetting balance" was used to measure the rate of wetting and to provide data used to calculate  $\gamma_{ls}$ , the liquid-solid surface tension. The wetting balance consists of a bottom loading balance accurate to 0.01 gram with a computer interface, a 1000°C top-loading furnace with a graphite crucible, and a lab jack that raises and lowers the furnace. In practice, a sample of the solid is suspended from the bottom of the balance and the liquid metal is melted in the furnace below the balance. When the solid sample and the molten metal are at the correct temperature for the test, the computer interface is activated to record the weight changes and the furnace is raised using the lab jack until the sample touches the liquid surface. At this time, an electrical circuit from the balance to the crucible is closed that deactivates the lab jack motor. This procedure allows for a reproducible (and small) penetration depth of the solid sample into the liquid so that buoyancy effects can be minimized. After 10 seconds the furnace was lowered and the sample was sectioned and metallographically examined to determine the thickness change.

Initial tests were performed to test the suitability of the methods on low melting point materials. Mild steel sheet was the solid sample and the 80Sn-20Pb solder was used as the molten metal. This alloy was chosen since it wets steel and melts at a temperature below 300° C.

The same equipment was used to measure the liquid-vapor surface tension ( $\gamma_{lv}$ ) using the drop weight method. A rod of the alloy was suspended vertically from the balance and the furnace was heated to 300°C for the solder alloy. The furnace was raised until just the end of the brazing rod was heated to its melting point and liquid drops formed and fell into the empty crucible. The weight change of the rod, which corresponds to the weight of the drop, was recorded for several drops and from these data,  $\gamma_{lv}$  was calculated.

### RESULTS & DISCUSSION

The data from a wetting balance test of steel and Sn80 solder at 300°C are presented in Figure 3. For the first three seconds the weight of steel sample was a constant 1.82 grams as the molten solder was being raised to contact the edge of the sample. The weight decreased rapidly at 3.19 seconds as the steel contacted the liquid solder and pushed down on the surface. There is no initial wetting and the steel formed a depression in the surface of the molten solder. The rate that the weight decreased is related to the speed at which

the solder pot is raised and the rate of wetting. The weight of the sample as it penetrates the surface of the molten solder does not reveal any surface tension data because it is dependent on many parameters such as the velocity of the solder pot and the shape of the solid sample edge.

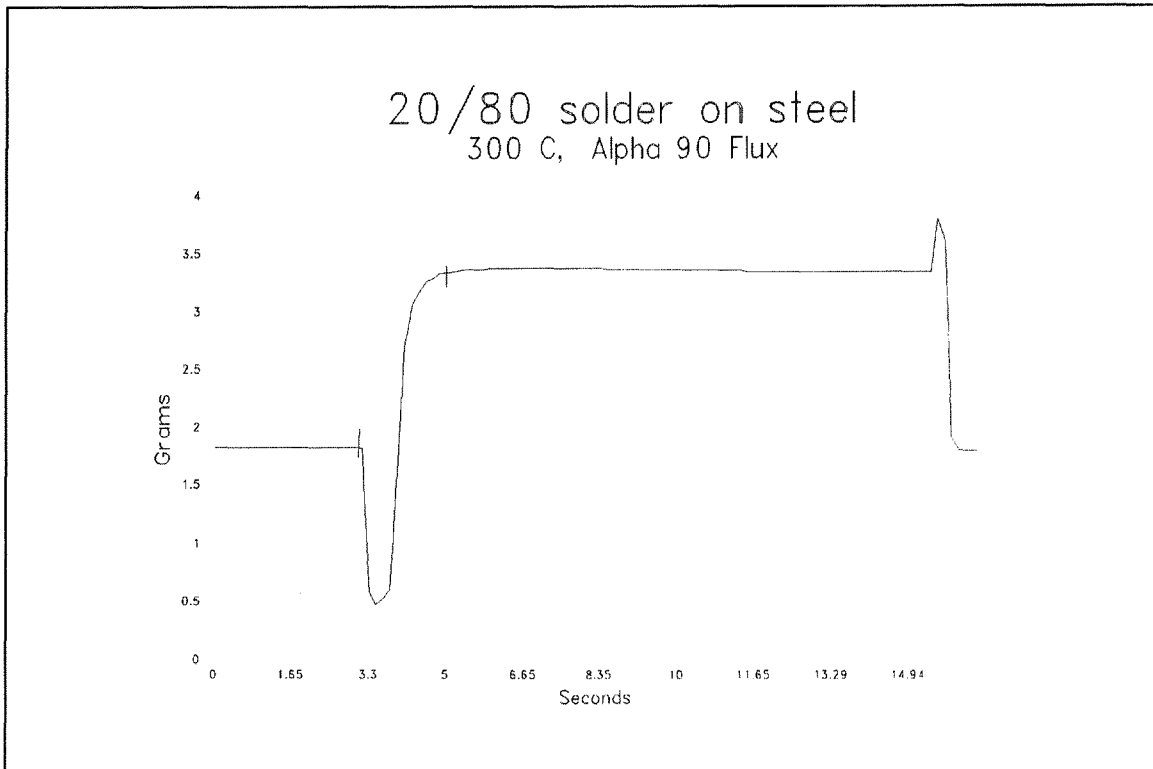


Figure 3. Wetting balance data for 80Sn-20Pb solder

The motor lifting the solder pot stopped when an electrical contact was made between the solder and sample, but inertia allowed the pot to rise a millimeter more after contact. Between 3.2 and 5.04 seconds, the solder wet the sample. During this time the molten metal reacted with any surface films on the steel and wet the solid. After five seconds the equilibrium meniscus formed and the weight leveled off at 3.37 grams and remains there until the solder pot was lowered at fifteen seconds. There is a spike in the weight of the sample as the liquid formed an inverted meniscus. The height of this spike is not relevant because the sample is in motion and equilibrium conditions do not apply.

The plot of weight versus time shows that the wetting time is approximately 2.2 seconds. This time represents the time from when the sheet of steel touched the molten solder surface to the time when the solder meniscus stopped advancing up the sheet. The change in weight due to the solder meniscus rising above the surface of the solder is 1.55 grams. The wetting angle was measured as  $0^\circ$  using an optical microscope at 100x so the value of  $\gamma_{ls}$  was calculated using equation 1 to be 245 dyne/cm.

Figure 4 is a plot of sample weight versus drop number during a pendant drop test. In this test a 80Sn-20Pb solder rod with a diameter of 0.32 cm and dipped in Kester SP-30 solder paste flux was used. The first drop weighed

0.15 grams and was most likely a drop of flux. All the remaining drops weighed between 0.25 and 0.27 grams. From these data,  $F$  was calculated from Equation 3 to be 0.2368, and the liquid-flux surface tension was calculated using Equation 2 to be 417 dyne/cm.

This compares with a literature value of 450 dyne/cm<sup>12</sup> but since they were measuring wetting in an inert gas while we were using a zinc chloride based flux, our value should be somewhat lower than the reported value. In a second test where no flux was used and the sample was surrounded by air, the value of  $\gamma_{LV}$  was determined to be 662 dyne/cm.

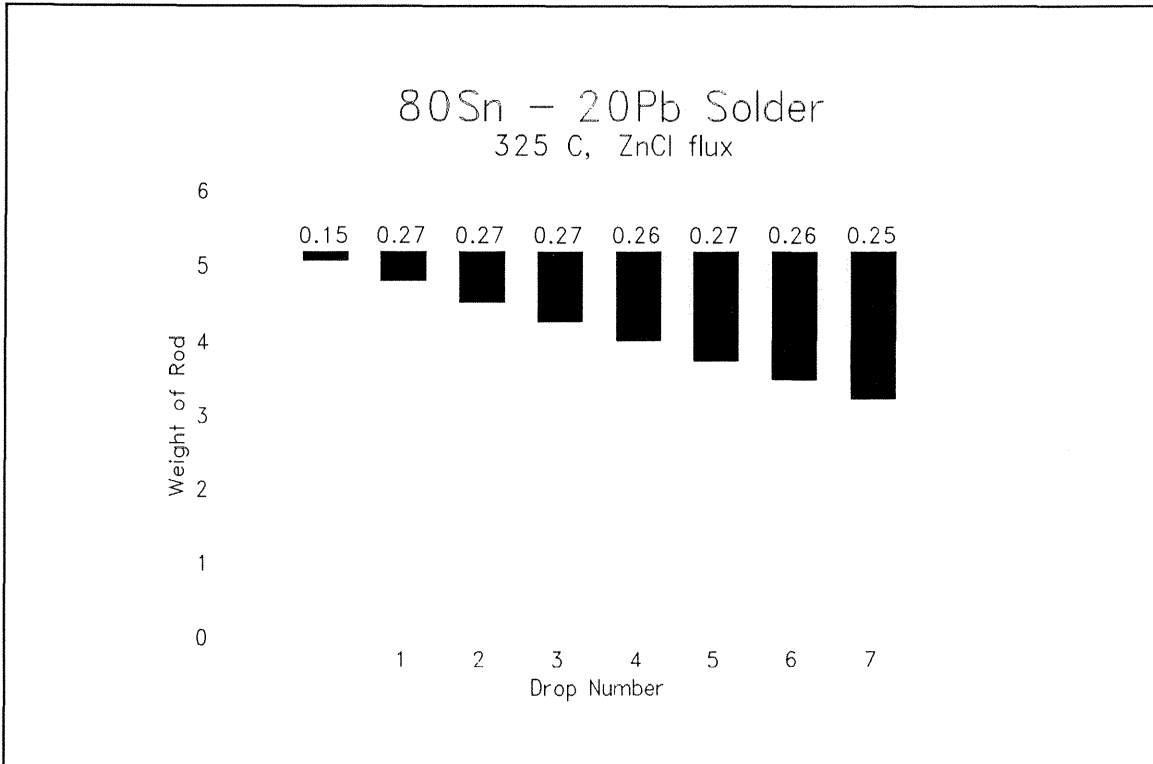


Figure 4. Data from pendant drop test on 80Sn-20Pb solder with flux

Without flux, the solder will not wet steel. Therefore, in order to determine the solid-vapor surface tension from Young's equation the liquid-vapor surface tension obtained using flux was used for this experiment. Because of this, the solid-vapor surface tension is actually the solid-flux surface tension. The contact angle  $\theta$  was measured from the cross section of the steel, and  $\gamma_{SV}$  was calculated using equation 4 to be 565 dyne/cm.

#### Summary

These techniques for measuring surface tension ( $\gamma$ ) and kinetic data are necessary to model the initial particle rearrangement stage of liquid phase sintering. The pendant drop technique is an accurate and reliable method of determining  $\gamma_{LV}$  and the wetting balance test gives not only  $\gamma_{LS}$ , but wetting kinetics data as well. By using this information we hope to be able to model the particle rearrangement process that occurs as the first stage in LPS. In

turn, the model of LPS will be used to optimize SLS of metal powders to make three dimensional parts.

This work is preliminary, to test the equipment and methods. Future work will include the surface temperature measurement of the brazing alloy in a reducing atmosphere.

#### Acknowledgements

This study was made possible by support from a State of Texas Advanced Research Project, ATP-116: Selective Laser Sintering: Direct Metal Fabrication and ONR grant #N00014-92-J-1314.

#### References

1. Kingery, W.D. "Densification during Sintering in the Presence of a Liquid Phase" J. Applied Physics 30 3, 301-306 (1959)
2. Gessinger, G.H., Fischmeister, H.F., and Lukas, H.L.; "A Model for Second-Stage Liquid-Phase Sintering with a Partially Wetting Liquid" Acta Met. 21 5, 715-724 (1974)
3. Courtney, T.H.; "Densification and Structural Development in Liquid Phase Sintering" 15A 6 1065-1074 (1984)
4. Huppmann, W.J. and Riegger, H.; "Modelling of Rearrangement Processes in Liquid Phase Sintering" Acta Met. 23 8, 965-971 (1975)
5. Kingery, W.D. and Berg, M. "Study of the Initial Stages of Sintering Solids by Viscous Flow, Evaporation-Condensation, and Self-Diffusion" J. Applied Physics 26 10, 1205-1212 (1955)
6. Huppmann, W.J. and Riegger, H.; "Modelling of Rearrangement Processes in Liquid Phase Sintering" Acta Met. 23 8, 965-971 (1975)
7. Kingery, W.D. "Densification during Sintering in the Presence of a Liquid Phase" J. Applied Physics 30 3, 301-306 (1959)
8. Vianco, P.T., Hosking, F.M. and Rejent, J.A.; "Solderability Testing of Kovar with 60Sn-40Pb Solder and Organic Fluxes" Welding Journal 6, 230s-240s (1990)
9. Lando, J.L. and Oakley, H.T.; "Tabulated Correction Factors for the Drop-Weight-Volume Determination of Surface and Interfacial Tensions" J. Colloid and Interface Sci. 25 526-530 (1967)
10. Murr, L.E.; Interfacial Phenomena in Metals and Alloys Techbooks p89-105 (1975)
11. Heady, R.B. and Cahn, J.W.; "An Analysis of the Capillary Forces in Liquid-Phase Sintering of Spherical Particles" Met. Trans. 1 1 185-189 (1970)

12. Murr, L.E.; Interfacial Phenomena in Metals and Alloys Techbooks p89-105  
(1975)